Theor Chem Acc (2011) 129:447–452
DOI 10.1007/s00214-010-0879-3

REGULAR ARTICLE

Theoretical study of the bent $U(\eta^8\text{-}C_8H_8)_2(CN)^-$ complex

Carine Clavaguéra · Jean-Pierre Dognon

Received: 27 October 2010 / Accepted: 16 December 2010 / Published online: 6 January 2011

Abstract The ground-state electronic structure of the cyanido complex $[U(\eta^8\text{-}C_8H_8)_2(CN)]^-$ as well as the thermodynamic properties and infrared spectrum are investigated using density functional theory including scalar relativistic effects. The complex is compared with the well-known uranocene $U(\eta^8\text{-}C_8H_8)_2$. Despite the broken symmetry, the gain in electrostatic interaction and a significant uranium-CN^- orbital interaction is sufficient to stabilize the bent CN^- complex with respect to uranocene. The formation of the CN^- complex is exothermic justifying the recently experimentally reported compound.

Keywords Actinide chemistry · Uranium · Metallocenes · Density functional calculations

1 Introduction

The possible existence of the uranium complex $U(\eta^8\text{-}C_8H_8)_2$ was suggested in 1963 by R. D. Fischer who noted that there might be "a possible additional gain in energy due to the participation of the f orbitals of heavy central atoms" [1]. The synthesis in 1968 of this first linear sandwich compound of an f element, by Streitwieser and Mueller-Westerhoff who christened uranocene to highlight its similarity with ferrocene [2, 3], was a milestone in the history of actinide chemistry [4, 5, 6]. It is now well established from spectroscopic properties [7, 8, 9] and theoretical analysis [10, 11, 12] that there is a significant metal–ligand bond covalence in uranocene with the participation of the 5f and 6d orbitals. This covalent stabilization and the inaccessibility of the metal center to supplementary ligands, due to steric constraints imposed by the two C_8H_8 rings, were invoked to explain the remarkable stability of uranocene, whose chemistry remained disappointingly poor. Especially, the lack of a $[U(\eta^8\text{-}C_8H_8)_2L]^{q-}$ complex (L = neutral or anionic ligand), whatever the charge, oxidation state and nature of the metal M, led to the generally accepted idea that a bis(η^8-C_8H_8) complex could not adopt a bent configuration, until the synthesis and X-ray crystal structure of $[M(\eta^8\text{-}C_8H_8)_2(CN)][NEt4]$ [13]. The suitable size and strong coordinating capacity of the cyanide ion obviously make it an efficient wedge for bending the linear uranocene.

Historically, the first work on $U(\eta^8\text{-}C_8H_8)_2$ including relativistic effects was done by Pyykkö et al. in 1981 [14] using relativistically parameterized extended Hückel calculations (REX). Few years later, Pitzer et al. provided information on the bonding in the ground-state and on the assignment of the visible spectrum from relativistic calculations including the spin–orbit interaction [15]. A large amount of mixing of the π ligand orbitals with the uranium 6d and 5f orbitals was found confirming expectation of a sizable covalent bonding. Dolg et al. performed large-scale ab initio multiconfiguration self-consistent field (MCSCF) and configuration interaction (CI) calculations in order to study the low-lying electronic states of the $M(C_8H_8)_2$

Dedicated to Professor Pekka Pyykkö on the occasion of his 70th birthday and published as part of the Pyykkö Festschrift Issue.

C. Clavaguéra (✉)
Laboratoire des Mécanismes Réactionnels,
Département de Chimie, Ecole Polytechnique,
CNRS, 91128 Palaiseau Cedex, France
e-mail: carine.clavaguera@dcmr.polytechnique.fr

J.-P. Dognon
CEA/SACLAY, UMR 3299 CEA/CNRS SIS2M,
Laboratoire de chimie de coordination des éléments f,
91191 Gif-sur-Yvette, France
e-mail: jean-pierre.dognon@cea.fr

(M = Nd, Tb, Yb, U) compounds [16]. For the uranocene complex, they confirmed the assignments of the ground state and first excited states previously made by Pitzer et al. and provided a more complete analysis for the higher states [15]. The role of the spin–orbit coupling was also evaluated for the uranocene. Very recently, Kaltsoyannis et al. performed all-electron spin–orbit coupled complete active space self-consistent field calculations including dynamic correlation via second-order perturbation theory (SOC-CASPT2) for the ground and low-lying excited states of $M(C_8H_8)_2$ (M = Th, U, Pu, Cm) [17]. In the uranocene case, they found that although the spin–orbit coupling induces very little differences on the equilibrium geometry, it had a significant effect on the energy spectrum. The uranocene ground state was found to be mainly a triplet $f_\pi^1 f_\phi^1$.

In this article, we report the theoretical investigation using density functional theory (DFT) of the electronic structure and bonding in the $U(\eta^8\text{-}C_8H_8)_2(CN)^-$ complex. The major question is "Can one explain why breaking the D_{8h} symmetry of the $U(\eta^8\text{-}C_8H_8)_2$, a stabilized bent geometry is obtained with the cyanide coordination?" Moreover, can one point out any specific reason to obtain the $U(\eta^8\text{-}C_8H_8)_2(CN)^-$ complex rather than the $U(\eta^8\text{-}C_8H_8)_2(NC)^-$ complex?

2 Computational details

Owing to the quasi mono-reference nature of the ground state [16, 17], we can expect that the DFT is an appropriate theoretical framework for the study of the $U(\eta^8\text{-}C_8H_8)_2(CN)^-$ complex. The geometries of the systems were optimized with the Amsterdam density functional (ADF) program [18, 19] using the OPBE functional that combines Handy's optimized exchange (OPTX) with the PBE correlation [20]. This functional was successfully employed by Kaltsoyannis et al. [21, 22] for the investigation of the electronic structure of actinide compounds.

The spin-unrestricted formalism was applied for the U system ($5f^2$). Both scalar and spin–orbit relativistic effects were considered using the zero-order regular approximation (ZORA) [23]. Slater-type orbitals (STOs) were employed as basis functions in SCF calculations. The TZ2P ZORA relativistic basis sets used have triple-ζ quality augmented by two sets of polarization functions. Within the ADF calculations, 14, 4, 5 and 1 explicit electrons were retained for U, C, N and H, respectively. Others were treated by the frozen core approximation. Vibrational frequencies were calculated to confirm that the structures are true minima on the potential energy surfaces.

The energy decomposition analysis (EDA) in the ADF program package is based on the work by Morokuma [24, 25] and Ziegler and Rauk [26]. The interaction energy ΔE_{int} is decomposed into electrostatic, Pauli repulsion and orbital mixing components:

$$\Delta E_{\text{int}} = \Delta E_{\text{elstat}} + \Delta E_{\text{Pauli}} + \Delta E_{\text{orb}}.$$

The estimated basis set superposition error is low at about 1% of the bonding energy of the $U(\eta^8\text{-}C_8H_8)_2(CN)^-$ complex.

The Voronoi deformation density (VDD) charges were calculated in order to evaluate the charge rearrangements due to the formation of the complex from the U^{4+}, $C_8H_8^{2-}$ and CN^- fragments. The VDD calculates the flow of electron density to or from a certain atom or fragment due to bond formation or charge rearrangements. This method does not explicitly use the basis functions. A description of the bonding was also performed in terms of bond orders. Many definitions have been proposed in the literature, but a known problem for the most popular bond indices is their basis set dependence. Recently, Ziegler et al. have demonstrated that the differential nature of the Nalewajski–Mrozek (N–M) bond indices makes them less sensitive to a basis sets effect [27]. The two-electron valence indices originally defined by Nalewajski and Mrozek have been derived from the changes in the two-electron density matrix due to the formation of the complex or molecule from isolated fragments. A deformation density (differential density) matrix, ΔP is defined as:

$$\Delta P = P - P^0$$

where P and P^0 correspond to the density matrices of the combined molecule (P) and the considered molecular fragments (P^0). In this work, we used the approach where the overall valence indice is obtained from the trace of the $P\Delta P$ matrix:

$$V = Tr\left[P^\alpha \Delta P^\alpha + P^\beta \Delta P^\beta\right]$$

where α and β are the spin variables of all electrons. The bond multiplicity is obtained from the valence indice by splitting the one-center index of an atom among the bonds that this atom forms. The bond multiplicity can be calculated as a sum of the relevant two-center part and weighted contributions from one-center indices of the two atoms. In the retained ADF implementation used in this study, the covalent two-center part is equal to the Gopinathan–Jug bond order (G–J) [28]. A detailed description of alternative valence indices and their physical meaning is summarized in Ref. [27].

In addition, supplementary information on chemical bonding was provided with an electron localization function (ELF) analysis of the ADF results with the DGrid 4.5 program package [29].

3 Results and discussion

3.1 Geometry and electronic structure

The π-sandwich $U(\eta^8\text{-}C_8H_8)_2$ complex is stabilized by the ligand–metal interactions and its D_{8h} symmetry. Thanks to the coordination of a cyanide ligand, the $U(\eta^8\text{-}C_8H_8)_2(CN)^-$ complex has been experimentally found to be a stable species [13]. The complex seems to be stabilized shifting to a bent conformation in spite of the loss of the D_{8h} symmetry. The structure of the $U(\eta^8\text{-}C_8H_8)_2(CN)^-$ complex and geometric parameters of both complexes are provided in Fig. 1 and Table 1, respectively. The computed U–C_8H_8 distances are in agreement with the experimental ones in both cases. However, the U–CN distance is shortened in DFT calculations by 0.1 Å. The C–N distance is similar to the experimental one in the free cyanide ion both in experiments and calculations [30]. As shown in experiments, the presence of the CN^- ligand leads to a complex with a bent coordination of the two C_8H_8 ligands. The Cnt-U-Cnt angle (Cnt = ring centroid) has a value of 151°, close to the experimental one of 153°.

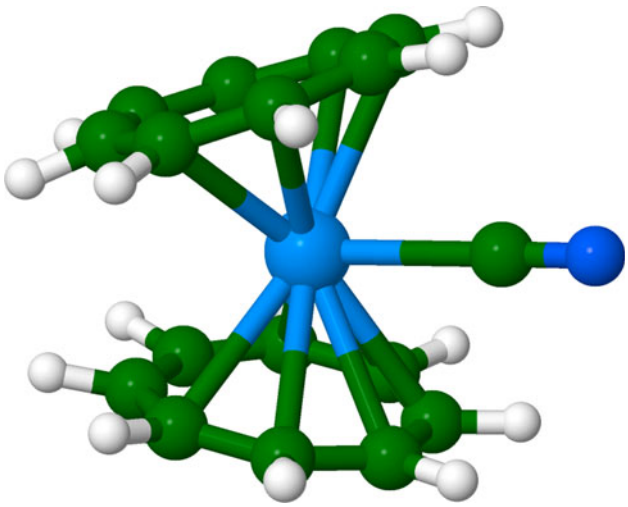

Fig. 1 DFT/OPBE optimized geometry of the $U(\eta^8\text{-}C_8H_8)_2(CN)^-$ complex

Table 1 Computed geometric parameters of the complexes in comparison with experimental data, distances are given in Å and angles in degrees (Cnt = centroid)

Complex	DFT	Exp
$U(\eta^8\text{-}C_8H_8)_2(CN)^-$		
d(U–CN)	2.53	2.63
d(C–N)	1.18	1.16
d(U–C_8H_8)	2.72	2.73
angle Cnt-U-Cnt	151	153
$U(\eta^8\text{-}C_8H_8)_2$		
d(U–C_8H_8)	2.62	2.65

The $U(\eta^8\text{-}C_8H_8)_2$ complex is energetically more stable than its parts with a large computed bonding energy of −2,039 kcal/mol. A comparison of the analysis of the electronic bonding energy of the $U(\eta^8\text{-}C_8H_8)_2$ and $U(\eta^8\text{-}C_8H_8)_2(CN)^-$ complexes is given in Table 2. The coordination of a CN^- ligand stabilizes the complex by 24 kcal/mol and increases the Pauli repulsion. However, this coordination is favorable thanks to electrostatic interactions with the U^{4+} ion, leading to a steric energy consisting of electrostatic plus repulsion contributions about 119 kcal/mol larger for the cyanide complex. The orbital interaction is large in both complexes but smaller in $U(\eta^8\text{-}C_8H_8)_2(CN)^-$ because of longer U-C_8H_8 distances. The electronic configuration of the $U(\eta^8\text{-}C_8H_8)_2(CN)^-$ complex is a $5f^2$ triplet. Previous multireference calculations on $U(\eta^8\text{-}C_8H_8)_2$ complex have shown that the $5f^2$ configuration dominates the low-lying states, namely uranocene is a U(IV) compound, i.e. a U^{4+} ion with a $5f^2$ configuration and two aromatic $C_8H_8^{2-}$ rings [16, 17]. The interaction with the CN^- ion does not modify this situation leading to the same conclusion for $U(\eta^8\text{-}C_8H_8)_2(CN)^-$. The higher spin-α valence molecular orbitals of the $U(\eta^8\text{-}C_8H_8)_2(CN)^-$ complex are represented in Fig. 2. The nature of the valence molecular orbitals was investigated through the symmetrized fragment orbital (SFO) analysis of the ADF results. Three distinct groups of molecular orbitals can be built. First, one group consists of localized molecular orbitals on the cyanide ligand (*A-46*) or on the uranium atom as pure 5f-orbitals (*A-52, A-53*). The second group is composed by U-C_8H_8 orbitals corresponding predominantly to interactions between the (C_8H_8) rings and the 6d and 5f uranium atomic orbitals (*A-43, A-44, A-48, A-50, A-51*). Finally, a third group can be constituted by orbitals that imply a participation of the cyanide ligand with uranium and the rings (*A-42, A-45, A-47, A-49*). The orbital *A-45* corresponds to a single CN^- participation mixed with 6d (3%) uranium orbitals. Orbitals *A-47* and *A-49* are formed by

Table 2 Bonding energy (BE) analysis at OPBE level starting from the U, $C_8H_8^{2-}$ and CN^- fragments

	$U(\eta^8\text{-}C_8H_8)_2(CN)^-$	$U(\eta^8\text{-}C_8H_8)_2$	$U(\eta^8\text{-}C_8H_8)_2(NC)^-$
BE	−2,063.48	−2,039.06	−2,058.30
Pauli repulsion	446.71	395.50	403.61
Electrostatic	−1,753.30	−1,582.99	−1,718.65
Steric	−1,306.59	−1,187.49	−1,315.05
Orbital	−756.89	−851.56	−743.25

Pauli + Electrostatic = Steric, Steric + Orbital = BE. All values in kcal/mol

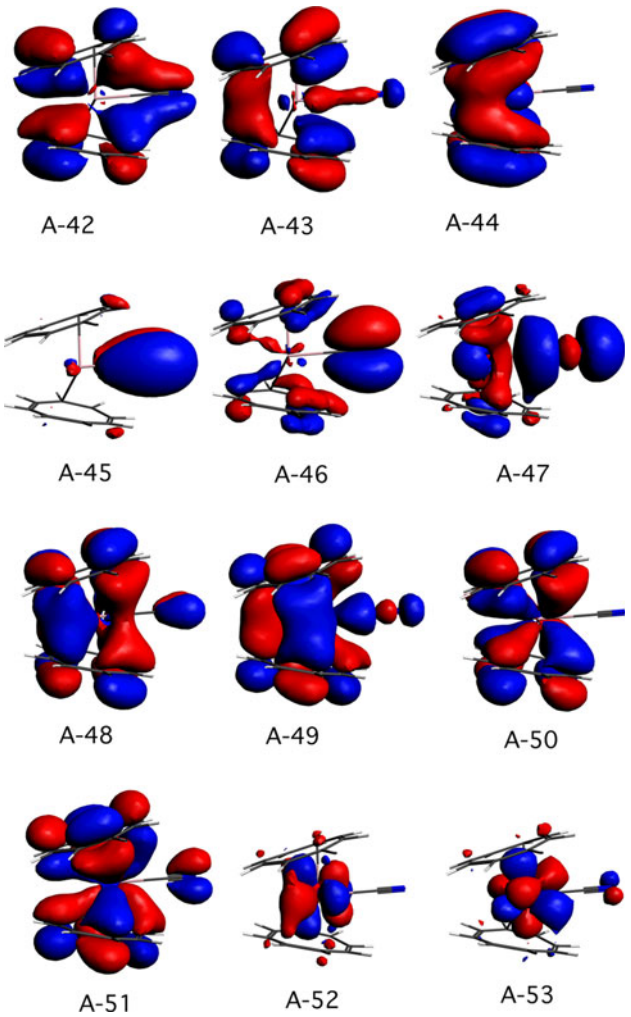

Fig. 2 Valence molecular orbitals for $U(\eta^8\text{-}C_8H_8)_2(CN)^-$ at DFT/OPBE level

a mixing of CN^-, (C_8H_8) and uranium orbitals with 6d (11%) and 5f (11%) + 6d (6%) participation, respectively. The orbital *A-42* presents an overlap between the cyanide ligand and uranium 6d (7%) and also between the cyanide and the C_8H_8 rings. This last group of molecular orbitals attests the role of orbital interaction in the stability of the $U(\eta^8\text{-}C_8H_8)_2(CN)^-$ complex with a large overlap between the CN^- ligand and the $U(\eta^8\text{-}C_8H_8)_2$ part.

Kaltsoyannis et al. [17] have shown that the geometry of the $U(\eta^8\text{-}C_8H_8)_2$ complex is unaffected by spin–orbit coupling. So, we can expect to have the same end result on the $U(\eta^8\text{-}C_8H_8)_2(CN)^-$ geometry. Nevertheless, the effects of spin–orbit splitting were investigated using a ZORA Hamiltonian with the ADF package. Including the spin–orbit coupling, the nature and the energetic order of orbitals involved in the interactions of the U^{4+} ion with the $C_8H_8^{2-}$ and the CN^- ligands are similar to the scalar relativistic ones. Thus, the bonding of uranium with CN^- is not influenced by spin–orbit effects.

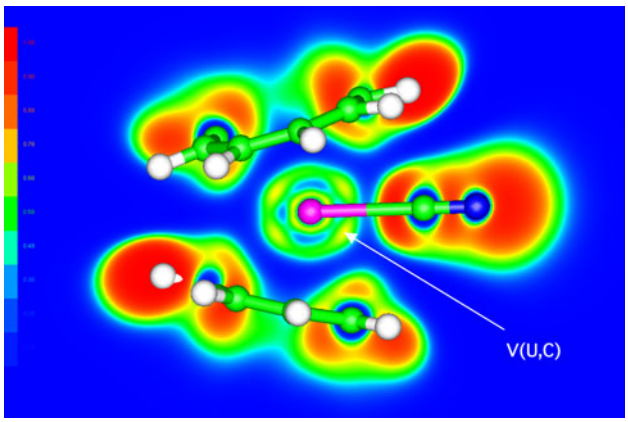

Fig. 3 Cut-plane ELF representation for the $U(\eta^8\text{-}C_8H_8)_2(CN)^-$ complex

The interaction properties between U and the CN^- can also be analyzed in terms of bond indices. The U–C interaction could be compared to a single bond with a G–J bond order and a N–M bond indices of 0.73 and 0.88, respectively. This is in agreement with the molecular orbital analysis discussed above where the participation of the uranium 6d and 5f orbitals is pointed out in the interaction with the CN^- ligand. These results support the hypothesis of a non-negligible covalent character in the U–C interaction. We should notice the expected triple bond character of the C–N bond (G–J bond order and N–M bond indices of 2.86 and 3.32, respectively).

The electron localization function provides a "picture" of the electronic structure showing the regions of the molecular space where the electrons localize. The local maxima of ELF define localization domains. The ELF function ranges from 0 (same spin pairs) to 1 (opposite spin pairs). To avoid any artifact, ELF was obtained from an all-electron calculation. The electronic ELF basin populations were derived from the integration of the total electron density. The interaction between the U^{4+} ion and the CN^- ligand is characterized by the formation of a V(U,C) basin with a population of 1.14 electrons. This is consistent with the results of the orbital analysis and can be observed in the 2D cut-plane picture (Fig. 3) where the ELF is plotted on a plane through $U\cdots C\cdots N$ atoms.

The VDD analysis exhibits a strong charge transfer to the U^{4+} ion. This electron transfer is mainly provided by the $C_8H_8^{2-}$ ligands ($\sim$1.3 e).

3.2 Chemical properties

3.2.1 Vibrational spectra

The DFT/OPBE-computed harmonic vibrational spectra are given in Fig. 4 for the $U(\eta^8\text{-}C_8H_8)_2$ and $U(\eta^8\text{-}C_8H_8)_2(CN)^-$

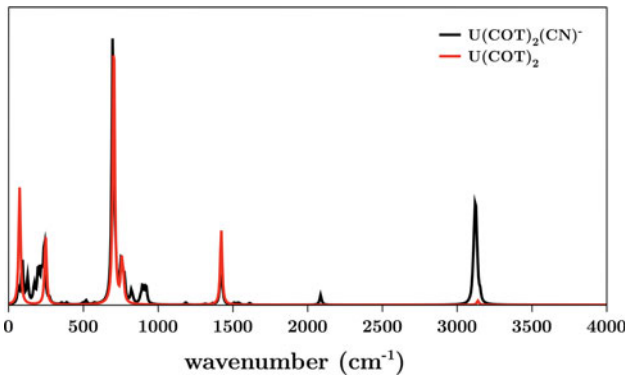

Fig. 4 Calculated harmonic vibrational spectra (cm^{-1}) for the $U(\eta^8\text{-}C_8H_8)_2$ and $U(\eta^8\text{-}C_8H_8)_2(CN)^-$ complexes without using a scaling factor. The calculated band intensities were convoluted assuming a Lorentzian profile with a full width at half maximum of $15\,cm^{-1}$

complexes. Due to the D_{8h} symmetry of $U(\eta^8\text{-}C_8H_8)_2$, several modes are IR inactive for this system. The spectra for both complexes are very similar with modes specific to the $U(\eta^8\text{-}C_8H_8)_2$ motif. The C–H stretch modes are clearly identifiable around $3,120\,cm^{-1}$, and the intensity of the band is stronger in the $U(\eta^8\text{-}C_8H_8)_2(CN)^-$ case. The band at $1,420\,cm^{-1}$ corresponds to the bend C–H modes. The very intense band at $700\,cm^{-1}$ and the band at $750\,cm^{-1}$ are characteristic of a mixing of C–H out of plane in (C_8H_8) and U-(η^8-C_8H_8) interaction modes. Two vibrational modes can be attributed to the presence of the cyanide ligand. The first one corresponds to the C–N stretch mode at $2,087\,cm^{-1}$ in good agreement with the experimental band at $2,073\,cm^{-1}$. The second one is the C–N out of plane mode at $920\,cm^{-1}$. It should be interesting to characterize the U–CN-specific mode as a fingerprint of the U–CN bond, but in our calculations this band occurs at around $240\,cm^{-1}$ and harmonic calculations are not accurate enough in this range due to strong anharmonic effects. However, far-IR experiments are not straightforward to carry out to obtain experimental data as reference.

3.2.2 *Estimation of the thermodynamic stability of the* $U(\eta^8\text{-}C_8H_8)_2(CN)^-$ *complex*

We considered the formation of the complex as a reaction described by the following equation:

$$U(\eta^8\text{-}C_8H_8)_2 + CN^- \rightarrow U(\eta^8\text{-}C_8H_8)_2(CN)^-$$

The reaction enthalpies and entropies for the formation of the $U(\eta^8\text{-}C_8H_8)_2(CN)^-$ complex were estimated from standard statistical thermodynamics (ideal gas assumed) after calculating DFT/OPBE harmonic vibrational frequencies. The calculated enthalpy ($\Delta_r H$) and Gibbs free energy ($\Delta_r G$) are -22 kcal/mol and -14 kcal/mol, respectively (T = 298.15 K and P = 1 atm). Accordingly, the formation of the complex under study is exothermic, confirming its thermodynamic stability.

3.3 The $U(\eta^8\text{-}C_8H_8)_2(NC)^-$ complex

The fact that the cyanide ion has similar good donor qualities at both its C and N atoms in general organic or organometallic chemistry makes interesting the study of both coordination types [31]. However, only the $U(\eta^8\text{-}C_8H_8)_2(CN)^-$ complex was experimentally obtained and we tried to understand and explain the differences with the $U(\eta^8\text{-}C_8H_8)_2(NC)^-$ complex. This point was never approached in the literature, while it was already observed experimentally for other uranium cyanide compounds [32]. From a general point of view, the interaction in the NC complex is less covalent due to a lowest participation of the U orbital to the bonding. For example, in the *A-47* orbital, the participation of the U(6d) orbital decreases to 7% in the NC complex. This effect is highlighted by a decrease in the bond order indices with G–J and N–M of 0.60 and 0.75, respectively. The analysis of the ELF function points out the formation of a V(U, N) basin with a population of 0.89 lower than the V(U, C) one in $U(\eta^8\text{-}C_8H_8)_2(CN)^-$ complex.

From an energetic point of view, the results of the energy decomposition analysis are presented in Table 2. The total bonding energy of the NC complex is not so different from that of the CN complex but ~ 5 kcal/mol in favor of the CN complex. Moreover, we observe larger differences by comparing each EDA term. The CN complex is more stabilized by the orbital interaction, which is consistent with our previous observations. The Pauli repulsion is larger in the CN complex that is also more stabilized by the electrostatic interaction.

4 Conclusions

The bent $U(\eta^8\text{-}C_8H_8)_2(CN)^-$ complex has been revealed to be chemically stable thanks to strong electrostatic and orbital interactions between the U^{4+} ion and the ligands. As previously found for the $U(\eta^8\text{-}C_8H_8)_2$ compound [14, 15], 6d, and to a less extend 5f, uranium orbitals have a significant participation in the interaction both with the aromatic rings and the cyanide ligand. The computed geometry and vibrational frequencies are close to the experimental ones recently obtained [13]. The ELF findings reinforce the idea of significant covalence between the U^{4+} ion and the CN^- ligand. Furthermore, the formation of the $U(\eta^8\text{-}C_8H_8)_2(NC)^-$ complex was found to be less

favorable with a lost of orbital interactions due to the nitrogen coordination. Hopefully, the present computational study will stimulate experimental investigations to prepare new bent $(\eta^8\text{-}C_8H_8)_2M$ complexes.

Acknowledgments We would like to thank Dr. Michel Ephritikhine for fruitful discussions and a careful reading of the manuscript.This work was granted access to the HPC resources of [CCRT/CINES/IDRIS] under the allocation i2010086146 made by GENCI (Grand Equipement National de Calcul Intensif).

References

1. Fischer RD (1963) Theor Chem Acta 1:418
2. Streitwieser A, Mueller-Westerhoff U (1968) J Am Chem Soc 90(26):7364
3. Streitwieser A, Mueller-Westerhoff U, Mares F, Grant CB, Morell D (1979) Inorg Synth 19:148
4. Marks TJ, Streitwieser A (1986) In: The chemistry of the actinide elements, vol 2, 2nd edn. Chapman and Hall, London, pp 1547–1571
5. Burns CJ, Eisen M (2006). In the chemistry of the actinide and transactinide elements, vol 5, 3rd edn. Springer, Netherlands, pp 2799–2910
6. Seyferth D (2004) Organometallics 23(15):3562
7. Harmon CA, Bauer DP, Berryhill SR, Hagiwara K, Streitwieser A (1977) Inorg Chem 16(9):2143
8. Brennan JG, Green JC, Redfern CM (1989) J Am Chem Soc 111(7):2373
9. Burns CJ, Bursten BE (1989) Comments Inorg Chem 9(2):61
10. Kaltsoyannis N, Bursten BE (1997) J Organomet Chem 528(1–2):19
11. Li J, Bursten BE (1998) J Am Chem Soc 120(44):11456
12. Parry JS, Cloke FGN, Coles SJ, Hursthouse MB (1999) J Am Chem Soc 121(29):6867
13. Berthet JC, Thuéry P, Ephritikhine M (2008) Organometallics 27(8):1664
14. Pyykkö P, Lohr LL (1981) Inorg Chem 20(7):1950
15. Chang AHH, Pitzer RM (1989) J Am Chem Soc 111(7):2500
16. Liu W, Dolg M, Fulde P (1997) J Chem Phys 107(9):3584
17. Kerridge A, Kaltsoyannis N (2009) J Phys Chem A 113(30):8737
18. Adf 2009.01, scm, theoretical chemistry, Vrije Universiteit, Amsterdam, The Netherlands, http://www.scm.com (2009)
19. te Velde G, Bickelhaupt FM, Baerends EJ, Guerra CF, van Gisbergen SJA, Snijders JG, Ziegler T (2001) J Comput Chem 22(9):931
20. Swart M, Ehlers AW, Lammertsma K (2004) Mol Phys 102(23):2467
21. Cavigliasso G, Kaltsoyannis N (2006) Dalton Trans 46:5476–5483
22. Cavigliasso G, Kaltsoyannis N (2007) Inorg Chem 46(9):3557
23. van Lenthe E, Ehlers A, Baerends EJ (1999) J Chem Phys 110(18):8943
24. Morokuma K (1971) J Chem Phys 55(3):1236
25. Kitaura K, Morokuma K (1976) Int J Quantum Chem 10(2):325
26. Ziegler T, Rauk A (1977) Theor Chem Acta 46:1
27. Michalak A, DeKock RL, Ziegler T (2008) J Phys Chem A 112(31):7256
28. Gopinathan MS, Jug K (1983) Theor Chem Acc 63:497
29. Kohout M (2009) Dgrid, version 4.5, radebeul
30. Hanusa TP, Burkey DJ (1994) In: King RB (ed) Encyclopedia of inorganic chemistry, vol 2. Wiley, Oxford, pp 943–949
31. Vahrenkamp H, Gei A, Richardson GN (1997) J Chem Soc, Dalton Trans 20:3643
32. Maynadié J, Berthet JC, Thuéry P, Ephritikhine M (2007) Organometallics 26(10):2623